

# Accepted Manuscript

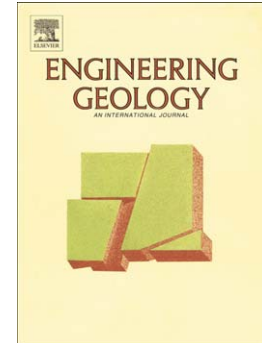
The role of graphite layers in gravitational deformation of pelitic schist

Shintaro Yamasaki, Masahiro Chigira, David N. Petley

PII: S0013-7952(16)30102-8  
DOI: doi: [10.1016/j.enggeo.2016.04.018](https://doi.org/10.1016/j.enggeo.2016.04.018)  
Reference: ENGEO 4270

To appear in: *Engineering Geology*

Received date: 17 August 2015  
Revised date: 1 February 2016  
Accepted date: 17 April 2016



Please cite this article as: Yamasaki, Shintaro, Chigira, Masahiro, Petley, David N., The role of graphite layers in gravitational deformation of pelitic schist, *Engineering Geology* (2016), doi: [10.1016/j.enggeo.2016.04.018](https://doi.org/10.1016/j.enggeo.2016.04.018)

This is a PDF file of an unedited manuscript that has been accepted for publication. As a service to our customers we are providing this early version of the manuscript. The manuscript will undergo copyediting, typesetting, and review of the resulting proof before it is published in its final form. Please note that during the production process errors may be discovered which could affect the content, and all legal disclaimers that apply to the journal pertain.

## The role of graphite layers in gravitational deformation of pelitic schist

Shintaro Yamasaki<sup>a</sup>, Masahiro Chigira<sup>b</sup>, David N. Petley<sup>c</sup>

<sup>a</sup>Corresponding author

Kitami Institute of Technology, Koen-cho 165, Kitami, Hokkaido 090-8507, Japan

E-mail: yamasaki@mail.kitami-it.ac.jp, TEL and FAX: +81-157-26-9481

<sup>b</sup>Disaster Prevention Research Institute, Kyoto University

Disaster Prevention Research Institute, Kyoto University, Gokasho, Uji Kyoto 611-0011,  
Japan

<sup>c</sup>School of Environmental Sciences, University of East Anglia, Norwich Research Park,  
Norwich NR4 7TJ, United Kingdom

### Highlights

- Microscopic slips in pelitic schist occur within thin graphite-rich layers.
- Continuous graphite layer has a considerable effect on shear resistance.
- Graphite rich zones are concentrated locally in pelitic schist area.
- Graphite rich zone could be important for the development place of landslide.

## Abstract

Deep-seated landslides in pelitic schists are common in many countries, but are poorly investigated and understood. In this study we present the first detailed examination and modelling of landslide mechanisms in these materials. We found that pelitic schist commonly contains black, graphite-rich layers on a scale of millimeters to centimeters thickness that are typically weaker than neighboring layers. By examining microscopic textures in borehole samples obtained from landslide masses of pelitic schist, we find that ductile gravitational shearing commonly occurs within these weaker layers, accompanied by brittle fracture in the surrounding layers. To investigate this mechanisms, we have performed high-precision direct shear tests, using a novel back-pressured shearbox, on artificial rock samples both with and without graphite layers placed between pre-cut shear surfaces. The tests used normal stresses up to 800 kPa (equivalent to 32 m depth of burial). We found that the coefficients of friction for samples with graphite layers embedded in the artificial rock samples (0.30, representing an angle of internal friction of  $16.7^\circ$ ) were much lower than those without graphite layers on the pre-cut surface (0.85). The shear strength of the artificial rocks with embedded layers of graphite decreased abruptly with increasing areal extent of the graphite layer along the shear surface, from which it can be inferred that the continuity of a graphite layer in natural pelitic schist has a considerable effect on shear resistance. These results suggest that even comparatively low dip angles of schistosity in pelitic schist could initiate microscopic slip along the graphite-rich layers.

**Key words**

landslide; deep-seated gravitational slope deformation; pelitic schist; graphite; shear strength

ACCEPTED MANUSCRIPT

## 1. Introduction

Landslides and deep-seated gravitational slope deformations in pelitic schist have occurred in many countries (Zischinsky, 1969; Chigira, 1992; Dramis and Sorriso-Valvo, 1994; Tibaldi et al., 2004; Hong et al., 2005; Ambrosi and Crosta, 2006; Yamasaki and Chigira, 2011). Whilst some of these landslides are the result of the susceptibility of schist to weathering, the largest slope failures occur because of deformation in bedrock. Pelitic schists are complex materials both mineralogically and in terms of structure, such that the mechanisms of failure in such situations are poorly investigated and understood.

Pelitic schist is formed during high P/T metamorphism; it exhibits well-developed schistosity and is therefore susceptible to shearing and thus to slope failure, particularly on dip slopes (Fujita et al., 1976; Chigira, 1992). Yamasaki and Chigira (2011) studied chemical weathering of pelitic schist and found that pyrite (a common constituent) has an important role in the generation of landslides. They showed that pyrite is oxidized at oxidation fronts to form sulfuric acid, which in turn dissolves rock-forming minerals and weakens the surrounding rocks. The slip surfaces of the landslides studied by Yamasaki and Chigira (2011) correspond to oxidation fronts, beneath which they observed fissile zones of dark pelitic schist that they interpreted to represent the incipient stage of small-displacement gravitational slope deformation. Graphite is a characteristic mineral of pelitic schist and is known to act as a solid lubricant (Oohashi et al., 2011; Rutter et al., 2013); the graphite is depleted in the oxidized zone but rich in the dark pelitic schist (Yamasaki and Chigira, 2011), so the mechanical properties of the schist in the fissile zone might be affected by the presence of graphite. However, we know of no previous studies that focus on the role of graphite in gravitational deformation and landslides in pelitic schist.

Although pelitic schist is susceptible to gravitationally-induced shearing and brittle fracture, there have been few *in situ* studies of structures in pelitic schist because of past difficulties in obtaining undisturbed fractured rock samples. However, we have examined undisturbed cores obtained from the Kurara and Zentoku landslides on Shikoku Island, Japan. The cores were obtained using a hybrid air-bubble drilling technique that uses both water and stiff-foam made from surfactant agent as cooling fluids (Takeda et al., 2006). Because stiff-foam fluids hardly penetrate fragile and permeable materials, such as are found in a shear zone, this technique preserves the fine structures formed by brittle deformation near the ground surface and provides almost 100% core recovery.

For this study, we undertook microscopic examination of pelitic schist samples from cores that had undergone gravitational slope deformation, and carried out simple shear tests on artificial graphite-bearing rock samples. We then considered the relationship between gravitational deformation and the initiation of landslides in pelitic schist.

## 2. Geologic setting

The landslides at Zentoku and Kurara occurred on slopes of pelitic schist and damaged houses, roads, and other infrastructure. The Zentoku landslide is composed of a lot of minor deep-seated rockslide blocks. The total area is as large as 1.8 km<sup>2</sup> (the maximum height is about 600 m, width is 2 km). The Kurara landslide is also composed of a lot of deep-seated rockslide blocks (Yamasaki and Chigira, 2011). One of blocks (about 5000 m<sup>2</sup>) moved and damaged infrastructures in 2000s.

The pelitic schist at the two sites formed within an accretionary prism and were then subjected to high P/T metamorphism at 90–60 Ma (Fig. 1, Isozaki et al., 2010). The original bedding planes of the sediments are parallel to the schistosity at both sites, and the dip of the schistosity corresponds to the direction of landslide movement. Work to mitigate the effects of slope failure has been undertaken at both sites. This work employed an advanced hybrid drilling technique to obtain samples that were used to identify rupture surfaces. Cores recovered from the landslide masses at these sites revealed a number of fragile fracture zones (Fig. 1) containing many voids, which suggests that the shearing developed close to the surface under low overburden pressures and was of non-tectonic origin. These zones represent brittle deformation and are clearly different from ductile synmetamorphic deformation indicated by flow folds. Active faults that can induce such brittle deformation under low overburden pressures have not been identified at or near the Zentoku and Kurara landslide sites (Nakata and Imaizumi, 2002).

The slip zones of these landslides lie immediately below an oxidation front and consist of black fractured rock that has been pulverized to silt size particles (Fig. 1). Polished surfaces coated with powdery graphite were observed in the fissile zone just below the slip zone of the Kurara landslide (Fig. 2) and webbed ruptures and ruptures along schistosity were developed along the boundaries of, or within, the black layers of pelitic schist (Fig. 1).

### 3. Methods

#### 3.1 Petrologic and mineralogic analyses

We prepared fourteen thin sections, which were cut normal to the schistosity in fractured pelitic schist samples. The sections were polished with 1  $\mu\text{m}$  diamond paste and examined microscopically under both transmitted and reflected light to identify opaque minerals, including graphite and pyrite.

Graphite was identified by X-ray diffraction analysis. Because the X-ray reflection spectra of other materials commonly overlap that of graphite, it can be difficult to identify graphite in rock samples. We extracted graphite from the samples by using the HF–HNO<sub>3</sub> dissolution method (Itaya, 1981) to allow us to detect the d(002) reflection, which is the strongest reflection for graphite. We used a Rigaku RAD-BII X-ray diffractometer with a Cu(K $\alpha$ ) target, an acceleration voltage of 40 kV, an electric current of 20 mA, and a scanning speed of 1°(2 $\theta$ )/min. Samples were scanned from 24°(2 $\theta$ ) to 28°(2 $\theta$ ).

We also identified graphite in carbonaceous components using a Perkin Elmer 2400 Series II elemental analyzer. To remove the carbon components of carbonates before elemental analysis, samples were reacted with HCl until bubbling ceased. Sulfur components in pyrite (FeS<sub>2</sub>) were determined with the same elemental analyzer.

A scanning electron microscope (Keyence VE-8800) was used to examine microscopic structures on joint surfaces, where graphite aggregates were assumed to have formed.

#### 3.2 Measurement of rock color and hardness

To examine the spatial variations of mineral composition and rock strength, we used rock color as an index of mineral composition, and hardness as an index of rock strength. Before taking measurements, cores of fresh pelitic schist were cut normal to schistosity and the cut surfaces were polished with ultra-fine emery paper (average particle diameter 10  $\mu\text{m}$ ). Eight 150 g samples of fresh rock were taken from the cores and powdered in an automated mortar mixer for 15 min. The polished core samples were used to measure rock color and hardness, and the powdered samples to measure rock color and for chemical analysis.

Rock color was measured by spectrophotometric colorimetry (Nagano and Nakashima, 1989, 1991; Yamasaki and Chigira, 2011) using a Konica-Minolta CM-2600d colorimeter with color values determined in the  $L^*a^*b^*$  color system, which is a three-dimensional coordinate system: the  $L^*$  axis defines brightness ranging from pure black (0) to pure white (100); the  $a^*$  axis defines the yellow–blue range from blue

(−50) to yellow (50); and the  $b^*$  axis defines the green–red range from green (−50) to red (50). The optical source for these measurements was D65 light (near sunlight); the field of view was  $10^\circ$ , and the diameter of the measuring window was 6 mm. The window was in direct contact with the surface of the polished rock or the compacted rock powder.

Rock hardness was measured with an Equotip hardness tester (Akashi AH401), which measures hardness within a narrow area of a surface by using a hemispherical impact hammer of 1 mm diameter. Impact velocities ( $V_i$ ) and rebound velocities ( $V_r$ ) are then used to calculate hardness expressed as  $1000 \times V_r/V_i$ . Hardness values range from 0 to 1000. Previous studies indicate that hardness correlates with unconfined compression strength for various rock types (Verwaal and Mulder, 1993; Aoki and Matsukura, 2008). Three hardness measurements were made in the same area for each sample and the values obtained were averaged. The impact surfaces for measurement were either the borehole core surfaces or polished cut surfaces.

### 3.3 Shear experiments on analogs of pelitic schist

The effects of shear and friction on graphite-bearing rocks were examined in experiments using artificial rock samples (analogous to pelitic schist) and a novel direct shear machine. Artificial samples were used because it is difficult to make a specimen with a specific layer to be sheared from natural pelitic schist; constituting layers of pelitic schist have some undulation and variations in thickness. The use of artificial samples allowed us to systematically analyze the effects on rock strength of different geometric relations between the graphite layers and the layers of other material, and to minimize the effects of sample variability.

Artificial rock samples containing graphite sheets were constructed as follows. The graphite sheet we used was a sealing material for industrial use (Klinger Graphite sheet HL, Klinger Ltd, UK). According to the specification from the supplier, the graphite sheet was made of crystallized graphite powder, the purity of which was greater than 98%, the sheet was made by mechanically compressing at pressures of 20–40 MPa into a density of about  $1 \text{ g/cm}^3$ . Since the true density of graphite is  $2.09\text{--}2.23 \text{ g/cm}^3$  (Anthony et al., 1990), the porosity of the sheet is about 50%. We have not examined the density of graphite in pelitic schist due to difficulty. But this graphite sheet exfoliate to small particles by friction with hand, and is similar to graphite in pelitic schist. The pressure of 20–40 MPa is quite greater than that of a slope inside. But pelitic schist underwent such pressure level underground. Thus it could be considered to be analogous to natural graphite layers of pelitic schist. The artificial rock material was made by mixing equal weights of plaster of Paris (dehydrated calcium

sulfate), quartz sand (grain size  $<1$  mm), and water, and then drying the mixture in rectangular block molds ( $100\text{ mm} \times 100\text{ mm} \times 10\text{ mm}$  and  $100\text{ mm} \times 100\text{ mm} \times 20\text{ mm}$ ) for 48 h under ambient room conditions.

Two series of shear tests were conducted (Fig. 3). Series I was designed to examine the frictional properties of the graphite sheet. For Series I, two 10-mm-thick blocks of plaster were sheared while in direct contact (Series I-A), and with a 5-mm-thick graphite sheet inserted between them (Series I-B). Before shearing, the surfaces of the plaster blocks and graphite sheets were abraded with medium-grade emery paper (average particle size  $200\text{ }\mu\text{m}$ ). Series II was designed to examine the shear properties of rocks with graphite sheets of different dimensions embedded within the sample on the shear plane, graphite sheets were embedded in molds using fixing slits on both sides of the mold: no graphite sheet (Series II-A), two graphite sheets each of  $5\text{ cm}^2$  area (Series II-B), two graphite sheets each of  $25\text{ cm}^2$  area (Series II-C), and two graphite sheets each of  $45\text{ cm}^2$  area (Series II-D). The surfaces of the graphite sheets used in the Series II tests were also abraded with medium-grade emery paper before the samples were constructed.

The direct shear machine we used was a Saturated/Unsaturated Back Pressured Shear box at Durham University (Brain *et al.* 2015). The shear displacement rate was  $0.1\text{ mm/min}$ . Normal stresses were 50, 100, 200, 400, and 800 kPa for series I, and 50, 100, and 200 kPa for series II, which reflect the ranges available for the machine.

## 4. Results

### 4.1 Mineralogy of pelitic schist and microfractures

The pelitic schist core samples we examined consist of thin whitish layers rich in quartz, muscovite, plagioclase, and chlorite, alternating with thin black layers rich in muscovite, chlorite, graphite, and pyrite. The thicknesses of whitish and black layers are in a scale of millimeters to centimeters. The black layers include very thin layers ( $<10\ \mu\text{m}$ ) of opaque minerals (Fig. 4), whereas the whitish layers contain no opaque minerals. The alternating sequence has been folded, with brittle fracture evident in the whitish layers, and ductile deformation in the thin layers of opaque minerals (Fig. 4A). Voids between quartz fragments in the whitish layers have been filled by material from the black layers, which was emplaced associated with disharmonic folding and flexural slip along the thin opaque mineral layers. Some open fractures in the whitish layers terminate at the boundaries of opaque mineral layers (Fig. 4B, C), which suggests that slip occurred at the boundary between the whitish and opaque mineral layers. These textural features indicate that microscopic slippage has occurred along the opaque mineral layers at shallow depth in response to gravitational slope deformation.

We identified graphite and pyrite as opaque minerals under the microscope with reflected light. Graphite grains have formed dimple depressions on polished surfaces because graphite has extremely low abrasion hardness. Pyrite grains are in the form of cubic crystals or framboidal aggregates within the opaque mineral layer (Fig. 4D; Uytenbogaardt and Burke, 1985).

X-ray diffraction profiles of the purified samples showed sharp  $d(002)$  reflection peaks that are typical of graphite (Fig. 5). The  $d$ -spacings for samples from the two landslide sites were slightly different, but were sharp in both cases. Concentrations of both carbon and sulfur showed reverse linear relationships with  $L^*$  of rock powder (Table 1, Fig. 6). That is, their concentrations were higher in the darker pelitic schist.

SEM images showed platy particles with shapes similar to those of graphite crystals on a mirror surface (Fig. 2B) that had a metallic luster similar to that of a graphite mass.

### 4.2 Rock color, strength, and composition relations

$L^*$  (brightness) and hardness ( $L$ ) were measured at 1-cm intervals along scan lines normal to the schistosity in polished core samples (Fig. 7A). The  $L^*$  and  $L$  profiles so obtained show very similar patterns; zones of low  $L^*$  also have low  $L$  values and these zones are mostly thick layers several tens of centimeters thick. A profile of  $L$  values

measured at 1-mm vertical intervals show that the thinly alternating black and whitish layers have higher  $L$  values than thicker black layers and have similar  $L$  values to those of whitish layers (marked “a” in Fig. 7B).

#### 4.3 Experiments on artificial rock samples

Shear stress-strain curves for all experiments are shown in Fig. 8 and peak strengths (Series I and II tests) and steady-state strengths (Series I only) are shown in Table 2.

The Series I tests were essentially ductile in behavior, although the tests at the highest normal loads showed a slight peak and residual style of behavior. The tests undertaken with a graphite sheet present (Series I-B) showed lower strength than those comprising of the artificial rock alone (Series I-A). Series I-A had a residual coefficient of friction of 0.85 (Fig. 9), corresponding to a friction angle of  $40.4^\circ$ , whilst the Series I-B had a corresponding friction coefficient of 0.30, corresponding to an angle of  $16.7^\circ$ . Thus the Series I tests showed that peak frictional strengths between artificial rock and graphite sheets were 35–55% of those between two artificial rocks, and that the steady-state frictional strengths between artificial rocks and a graphite sheets were 31–45% of those between two artificial rocks. This is not a surprising result, given the known low strength of graphite (typically  $\theta = 8 - 16^\circ$  according to Hoek and Brown 1980).

For Series II tests, the shear strength of the samples depended strongly on the relative proportions of graphite and the artificial rock (Fig. 10). This effect was particularly significant when the proportion of the graphite layer exceeded 50%, beyond which the shear strength reduced dramatically irrespective of normal stress. Thus, sample type II-D, which had graphite sheets of total area  $90 \text{ cm}^2$  embedded on the shear plane, showed considerably lower strengths than the other samples at normal stresses of 50, 100, and 200 kPa. After the shear tests, a number of irregular fractures had formed oblique to the shear plane in the type II-A samples (no embedded graphite sheet), II-B ( $10 \text{ cm}^2$  of graphite sheet), and II-C ( $50 \text{ cm}^2$  of graphite sheet), but the fractures formed in type II-D samples were connected smoothly to the two graphite sheets (Table 2, Fig. 11).

## 5. Discussion

Our microscopic examination of gravitationally deformed pelitic schist suggests that the deformation is closely associated with the areal extent of the black layers (a scale of millimeters to centimeters) in the shear plane; the black layers are inherited from the argillaceous protolith. We observed evidence of ductile deformation and slippage along black layers, accompanied by brittle fracture of neighboring whitish layers and intrusion of black layers into the numerous voids formed by the fractures. The opening of similar fractures has been reported by Chigira (1985) in near-surface gravitationally deformed pelitic schist, which supports the view that the deformation occurred near the ground surface, presumably in response to gravitational slope deformation. The black layers contain many thin layers ( $<10\ \mu\text{m}$ ) of opaque minerals (Fig. 4); increasing darkness of the rock corresponds to higher concentrations of both carbon and sulfur (Fig. 6). The brightness ( $L^*$ ) of the rock increases as carbon content decreases during weathering (Yamasaki and Chigira, 2011). The pelitic schist we examined originates from deep-marine muddy sediments that were metamorphosed within an accretionary complex such that the graphite in the pelitic schist was derived from marine organic material. Framboidal aggregates of pyrite (Fig. 4D) are common in argillaceous deposits and are genetically related to sulfur bacteria (Wilkin and Barnes, 1997).

The thickness of the black layers in the pelitic schist may be determined by the original layering of organic-rich material or may reflect segregation during metamorphism. Carbonaceous material in mudstone is transformed into graphite during metamorphism (Landis, 1971; Itaya, 1981; Nakamura, 1995). Graphite formed at high temperatures and high pressures exhibits strong crystallinity and has large  $d(002)$  spacings (Nakamura, 1995). The  $d$ -spacings that we determined (Fig. 5) are consistent with the results of Nakamura (1995), who reported that the  $d(002)$  spacings of graphite range from 0.3357 nm ( $26.55^\circ(2\theta)$ ) to 0.3450 nm ( $25.8^\circ(2\theta)$ ) and that the half width of graphite  $d(002)$  reflections ranges from  $0.17^\circ$  to  $2.60^\circ(2\theta)$  in the Daimonji contact aureole east of Kyoto in Japan.

Our experiments showed that the presence of graphite in a shear plane reduces friction during shear. We showed that the peak and steady-state frictional strengths between graphite sheets and artificial rock samples were much lower than those between the two artificial rocks, suggesting that the graphite-rich black layers in pelitic schist are sheared more easily than the whitish layers without graphite. The steady-state frictional strength of joints in our artificial rock samples was about 0.83

times that of the normal stress applied. This result conforms with Byerlee's law, which states that for normal stress of  $<200$  MPa the frictional strength within rock joints is about 0.85 times the normal stress applied; Byerlee's law is applicable to various rock types (Byerlee, 1978; Scholz, 2002). However, the frictional strengths that we determined between graphite sheets and artificial rock samples were, on average, about 0.30 times the normal stress (Fig. 9); thus, the presence of a graphite layer reduced friction.

As we mentioned, graphite is an effective solid lubricant and its coefficient of friction and separation energy are smaller than other rock-forming minerals (Morrow et al., 2000). Savage (1948) suggested the lubricity is effective in an atmosphere containing oxygen or water vapor. Recent studies stated that the lubricity of graphite is effective in both dry and wet condition. Morrow et al. (2000) reported the coefficient of friction is around 0.15 in dry and wet conditions, and Rutter et al. (2013) reported about 0.1 in wet conditions. Landslides in nature usually occur under wet conditions and the groundwater is frequently oxidizing, which are favorable conditions of reducing friction. In addition, the lubricity of graphite increases with increasing crystallinity and purity of the graphite (Grattan and Lancaster, 1967). The crystallinity of the graphite in the pelitic schist that we examined was high, as indicated by sharp  $d(002)$  X-ray reflections (Fig. 5). Although graphite grains are very small and scattered in black layers, they can be smeared and interconnected when pelitic schist is sheared along schistosity, forming a mirror surface as shown in Fig. 2. The shear resistance of rock could thus be decreased with shearing.

If a number of closely spaced graphite-rich layers are sheared, they undergo ductile deformation, whereas brittle fracture would occur in the juxtaposed layers with lower graphite present, forming voids into which the black layers are thrust during flexural slip folding (Fig. 4A).

The continuity of graphite layers within rocks also has an important influence on rock strength. We showed that the peak strength of artificial rock samples containing embedded graphite sheets of  $90 \text{ cm}^2$  area (90% of the area of the experimental shear surface; test II-D) was low for all normal stress conditions tested (Fig. 8). Moreover, the type II-D samples were the only ones to exhibit singular smooth rupture surfaces after shearing (Table 2).

For type II-D samples, shear stress under normal stress of 50 kPa increased sharply in the early stage of shearing, but the increase was more gradual under normal stresses of 100 and 200 kPa (Fig. 8). This slower, creep-like initial deformation under higher normal stresses may suggest that the effects of slip within the graphite layers

appeared at an earlier stage than in the tests at lower (50 kPa) normal stress. This reason is still unknown, but higher normal stress conditions may induce ductile deformation of graphite and decrease shear resistance.

There was considerably less dilatation of fractures after the shear tests under normal stresses of 100 and 200 kPa than for the tests under normal stress of 50 kPa. This outcome is consistent with our observation of smooth rupture surfaces formed in shear tests under higher normal stresses (Table 2). Strictly speaking, the graphite grains in pelitic schist are non-contiguously distributed, even though they may be concentrated in a thin layer. Mechanical shearing of the black layers in pelitic schist would start with shear surfaces connecting graphite grains and gradually the whole shear surface is smeared with graphite.

Our experiments showed that shear stresses for the graphite-embedded rocks had not reached steady-state conditions after 10 mm of shear displacement; shear stress was still decreasing, albeit only slightly. Type II-D samples showed the lowest shear stresses and these approached the residual stresses obtained in the shear tests of the graphite layer (test I-B), which suggests that shearing of the type II-D samples resulted in smearing of graphite over the entire shear plane. The relation between the areal extent of the graphite layer on the shear surface and peak strength in our experiments was not linear. Strength decreased abruptly when we increased the areal extent of the graphite layer from 50% to 90% of the area of the experimental shear plane, particularly for tests under normal stresses of 100 and 200 kPa. This difference in behavior may reflect differences in the stress distributions in rock matrices and graphite layers; under high normal stress, rock matrices may be able to withstand greater shear stress than graphite because graphite is much less rigid than rock. This contention is supported by our finding that, under normal stress of 200 kPa, the peak strength of samples with an embedded graphite layer of 50 cm<sup>2</sup> area was only slightly greater than the peak strength of samples with a graphite layer of 10 cm<sup>2</sup> area. Nonetheless, our experiments showed that further increase of the areal extent of the graphite on a shear surface dramatically decreased the peak shear strength.

The stress paths for all tests in Series II did not reach a steady-state. If samples of Series II were completely pulverized by long enough shear displacement, shear strength could reach it. A friction coefficient and cohesion of a pulverized material of artificial rock is an eventual material property at steady-state stage. We did not examine them for the pulverized material of the artificial rock. However, they could be larger than graphite. For example, Oohashi et al. (2013) showed that the coefficient of friction of angular quartz (<200  $\mu\text{m}$ ) is around 0.6 under normal stresses of 2 MPa and

at slip rate of 0.00020 m/s which is close to the shear rate of our experiments.

Rutter et al. (2013) used friction experiments with graphite powders to show that the coefficient of friction of pure graphite is around 0.1 ( $\phi=5.7^\circ$ ) under normal stresses of 3, 50, 100, and 150 MPa. They used graphite powder samples in a direct shear apparatus and sandwiched between facing blocks of rock in a standard triaxial shear apparatus. Oohashi et al. (2013) also showed around 0.1 under normal stress of 2 MPa with powdered graphite by a shear apparatus using facing rotating cylinder rocks. In our series I experiments, however, we found the coefficient of friction between graphite sheets and the artificial rock to be around 0.3 ( $\theta = 16.7^\circ$ ) under normal stresses of less than 800 kPa. The friction coefficients may be attributed to the difference in graphite form. Mechanically pressed sheets of graphite and artificial rocks probably have small asperities of quartz grains in the surface of the artificial rock samples, which might have impeded slip.

Our experiments were for planar shear surfaces using artificial rock plates and graphite sheets, while natural pelitic schist has generally undulating schistosity in microscopic scale and graphite grains are distributed in black layers. These must be considered to compare the results of our experiments and natural gravitational slope deformation. Ideally, our experiments suggest that a rock slope containing a continuous graphite layer with a downslope dip steeper than  $16.7^\circ$  (frictional coefficient, 0.3) would slide. On the other hand, graphite layers in pelitic schist are not continuous and minor folding and crenulation of the schistosity interfere the slip along schistosity plane. However, if microscopic slip along graphite layers occurred and led to stress concentration at the salients of whitish layers, slip along graphite grains and its smearing would proceed and fragments of silicate minerals and graphite would become a mixture. Silicate minerals may be fractured under the influence of subcritical crack growth, which is dependent on both time and the local environment (Atkinson, 1984). Fracturing of silicates proceed slowly depending on time, slips on graphite layer are likely to help shearing of whole rock.

Graphite sheet thickness we took was 5 mm, which was thick enough for our experiments, because the artificial rock surfaces on both sides of a graphite sheet did not contact after the shear experiments.

The experiments we carried out were quite smaller scale and took much shorter time than real gravitational deformations, and there are many differences in terms of materials, structures, and time constants. Undulations of pelitic schist may be on the order of slope scale in nature and natural gravitational slope deformation proceeds very slowly (Ambrosi and Crosta, 2006). The latter fact may lead to a large

strength reduction of rocks (Itô and Sasajima, 1987). To consider the occurrences of real gravitational deformation in pelitic schist, chemical processes also should be discussed. Chemical reactions involving sulfuric acid derived from oxidation of pyrite may also play an important role in the evolution of a slip zone. Yamasaki and Chigira (2011) suggested that these reactions are an important process in the weathering of pelitic schist as sulfuric acid would break or weaken chemical bonds within the schist. Graphite and pyrite commonly occur together, so it is possible that oxidizing water may penetrate a rock through fractures caused by slip along graphite layers within it, resulting in the formation of sulfuric acid that weakens chemical bonds in neighboring minerals.

## 6. Conclusions

Pelitic schist, a rock type that is prone to gravitational slope deformation and landslide, is generally composed of black layers that are rich in muscovite, chlorite, graphite, and pyrite, interlayered with whitish layers rich in quartz, muscovite, plagioclase, and chlorite. Gravitational deformation of pelitic schist is associated with ductile slip along the black layers and brittle fracture of the whitish mineral layers. Slip within the black layers is attributed to the lubricating properties of graphite, of which the content increases with increasing darkness of the rock. Simple shear tests along pre-cut surfaces of two pieces of artificial rock, with and without graphite sheets between them, and other tests on artificial rocks with graphite sheets embedded on the shear plane, revealed that increasing the areal extent of the graphite sheet reduced shear strength. In particular, when the areal extent of the graphite sheet reached about 90% of the experimental shear plane, there was a rapid decrease in shear strength.

From the results of our experiments it can be inferred that during shearing along schistosity of natural pelitic schist, graphite is smeared on the neighboring rock surfaces and dramatically reduces frictional resistance. Because the graphite in pelitic schist is derived from organic-rich sediment, one of the effects of metamorphism is to concentrate it in discrete horizons. If the schistosity of such graphite-rich layers is exposed downslope, shearing within the schistose layers is likely to initiate gravitational slope deformation and landslide.

## Acknowledgements

Core from the Zentoku landslide site was acquired by Nippon Koei Co., Ltd. for the Bureau of Erosion Control for the Shikoku mountainous area. Core from the Kurara landslide site was acquired by Japan Conservation Engineers and Co., Ltd. for the Kawashima Agriculture and Forest Office of the Tokushima Prefectural Government. We subsampled the core from both sites with assistance from the organizations that acquired them. E. Nakata and T. Wakamatsu (Central Research Institute of Electric Power Industry) assisted us with our use of the elemental analyzer. A. Suemine (Disaster Prevention Research Institute of Kyoto University) provided useful information about the landslides for our study. M. Brain, A. Clark, S. Waugh, and C. Longley (Department of Geography, Durham University) assisted with shearing tests. This research was supported by Grants-in-Aid for Scientific Research (No. 08J00578 to S.Y. and No. 23310126 to M.C.) and a Grant-in-Aid from Fukada Geological Institute.

## Captions

### Figure 1

Structures in cores drilled vertically through pelitic schist landslides at Kurara and Zentoku and photographs and interpretive sketches of slip zones and open fractures. Locations of thin-sections in Fig. 4 are also shown. Map showing Sanbagawa and Shimanto high P/T metamorphic zone is modified from Isozaki et al. (2010).

### Figure 2

(A) Photo of graphite-smear surface, which is assumed to be a preliminary sliding surface, in the fissile zone below a shear plane of Kurara landslide (location shown in Fig. 1) and (B) secondary electron image of the mirror surface.

### Figure 3

Design of analog experiments used to simulate friction and shear behavior of graphite-bearing rock.

### Figure 4

Thin-section photographs showing microscopic slips and folds in pelitic schist from Kurara and Zentoku landslide sites. (A) Micro-fold in layers of mica and chlorite interleaved with layers of opaque minerals (red arrows). Mica and chlorite layers have been thrust between two rotated quartz fragments in a layer of fractured quartz. Folding was caused by flexural slip along opaque mineral layers. (B) Open fractures in quartz-chlorite-mica layers. Fractures terminate at black layers; some show evidence of slip along the black layers (red arrows). (C) Open fractures within a thin continuous layer of opaque mineral. (D) Close-up view of area marked by square in photo C under plane-polarized light (left) and reflected light (right). Qtz, quartz; Ms, muscovite; Chl, chlorite; Pl, plagioclase; Py, pyrite; FPY, framboidal pyrite; Sp, sphene; D, dimple depressions in graphite domains. Photos A, B, and C (locations shown in Fig. 1) taken under transmitted plane-polarized light.

### Figure 5

Results of X-ray diffraction analysis of pelitic schist from the Kurara and Zentoku landslide sites. The graphite d(002) reflection is clearly shown. Gr, graphite; Tur, tourmaline; Ilm, ilmenite; Rt, rutile.

## Figure 6

Relationships of  $L^*$  of powdered pelitic schist with concentrations of carbon (solid circles) and sulfur (open circles).  $L^*$  values were measured by spectrophotometry, indicates brightness ranging from pure black (0) to pure white (100).

## Figure 7

Core photos showing petrologic texture, and variations in hardness ( $L$ ) and brightness ( $L^*$ ) in a core from the Zentoku landslide site.  $L$  values were measured by Equotip hardness tester, range from 0 to 1000 with increasing hardness. The  $L^*$  value were measured by spectrophotometry; it ranges from pure black (0) to pure white (100). (A) Vertical profiles of brightness and hardness measured at 1-cm intervals. (B) Polished surface of pelitic schist obtained from 23.5 m depth with hardness profile measured at 1-mm intervals. The sequence of thin alternating layers of black and whitish layers (marked “a”) is considerably harder than the thick black layer (marked “b”).

## Figure 8

Shear stress curves at various normal pressures for all shear tests.

## Figure 9

Relations of peak and steady-state frictional strength with normal stress in shear tests with and without graphite layers. Slopes of lines of best-fit are average coefficients of friction at steady state.

## Figure 10

Relation of peak frictional strength with areal extent (percent of area of shear plane) of graphite layer embedded in the shear plane of artificial rock samples at various normal stresses.

## Figure 11

Examples of the samples after shear tests. GS: graphite sheet.

## References

- Ambrosi, C., Crosta, G., 2006. Large sackung along major tectonic features in the Central Italian Alps. *Engineering Geology* 83, 183-200.
- Anthony, J.W., Bideaux, R., Bladh, D., Nichols, M.C., 1990. *Handbook of Mineralogy*.

- Volume I. Elements, Sulphides, Sulphosalts. Mineral Data Publishing, Tucson.
- Aoki, H., Matsukura, Y., 2008. Estimating the unconfined compressive strength of intact rocks from Equotip hardness. *Bulletin of Engineering Geology and the Environment* 67, 23-29.
- Atkinson, B.K., 1984. Subcritical crack growth in geological materials. *Journal of Geophysical Research: Solid Earth* 89, 4077-4114.
- Brain, M.J., Rosser, N.J., Sutton, J., Snelling, K., Tunstall, N. & Petley, D.N. 2015. The effects of normal and shear stress wave phasing on coseismic landslide displacement. *Journal of Geophysical Research: Earth Surface*. 120:1009–1022.
- Byerlee, J., 1978. Friction of rocks. *Pure and Applied Geophysics* 116, 615-626.
- Chigira, M., 1985. A large mass rock creep structure of crystalline schist at Ogai district in the Sambagawa terrain in the Kanto mountainous land. *Journal of Geography (Chigaku Zasshi)* 94, 357-380. (in Japanese with English abstract)
- Chigira, M., 1992. Long-term gravitational deformation of rocks by mass rock creep. *Engineering Geology* 32, 157-184.
- Dramis, F., Sorriso-Valvo, M., 1994. Deep-seated gravitational slope deformations, related landslides and tectonics. *Engineering Geology*, 38, 231-243.
- Grattan, P., Lancaster, J., 1967. Abrasion by lamellar solid lubricants. *Wear* 10, 453-468.
- Fujita T, Hirano M, Hada S. 1976. The Structural Control of Landslides in the Kawai Area, Tokushima Prefecture, Shikoku. *Landslides - Journal of the Japan Landslide Society* 13, 25-36. (in Japanese with English abstract)
- Hong, Y., Hiura, H., Shino, K., Sassa, K., Suemine, A., Fukuoka, H., Wang, G., 2005. The influence of intense rainfall on the activity of large-scale crystalline schist landslides in Shikoku Island, Japan. *Landslides* 2, 97-105.
- Isozaki, Y., Aoki, K., Nakama, T., Yanai, S., 2010. New insight into a subduction-related orogen: a reappraisal of the geotectonic framework and evolution of the Japanese Islands. *Gondwana Research*, 18, 82-105.
- Itaya, T., 1981. Carbonaceous material in pelitic schists of the Sanbagawa metamorphic belt in central Shikoku, Japan. *Lithos* 14, 215-224.
- Itô, H., Sasajima, S., 1987. A ten year creep experiment on small rock specimens. *International Journal of Rock Mechanics and Mining Sciences & Geomechanics Abstracts*, 24(2), 113-121.
- Landis, C., 1971. Graphitization of dispersed carbonaceous material in metamorphic rocks. *Contributions to mineralogy and petrology* 30, 34-45.
- Morrow, C., Moore, D.E., Lockner, D., 2000. The effect of mineral bond strength and adsorbed water on fault gouge frictional strength. *Geophysical Research Letters*,

- 276, 815-818.
- Nagano, T., Nakashima, S., 1989. Study of colors and degrees of weathering of granitic rocks by visible diffuse reflectance spectroscopy. *Geochemical Journal* 23, 75-83.
- Nagano, T., Nakashima, S., 1991. A convenient method of color measurement of marine sediment by colorimeter. *Geochemical Journal*, 25, 187-197.
- Nakamura, D., 1995. Comparison and interpretation of graphitization in contact and regional metamorphic rocks. *Island Arc*, 4, 112-127.
- Nakata, T., Imaizumi T., 2002. Digital active fault map of Japan. University of Tokyo Press, Tokyo. in Japanese
- Oohashi, K., Hirose, T., Shimamoto, T., 2011. Shear-induced graphitization of carbonaceous materials during seismic fault motion: Experiments and possible implications for fault mechanics. *Journal of Structural Geology* 33, 6, 1122-1134.
- Oohashi, K., Hirose, T., Shimamoto, T., 2013. Graphite as a lubricating agent in fault zones: An insight from low - to high - velocity friction experiments on a mixed graphite - quartz gouge. *Journal of Geophysical Research: Solid Earth*, 118(5), 2067-2084.
- Rutter, E.H., Hackston, A.J., Yeatman, E., Brodie, K.H., Mecklenburgh, J., May, S.E., 2013. Reduction of friction on geological faults by weak-phase smearing. *Journal of structural geology* 51, 52-60.
- Savage, R.H., 1948. Graphite lubrication. *Journal of applied physics* 19, 1-10.
- Scholz, C.H., 2002. *The mechanics of earthquakes and faulting*, 2nd edition. Cambridge University Press, Cambridge.
- Takeda, S., Komiya K., Takeuchi, I., 2006. From air bubble boring: the hybrid method to a core sampling system of high quality: *Journal of the Japanese Geotechnical Society (Tsuchi-to-Kiso)*, 54, 16-18. (in Japanese)
- Tibaldi, A., Rovida, A., Corazzato, C., 2004. A giant deep-seated slope deformation in the Italian Alps studied by paleoseismological and morphometric techniques. *Geomorphology* 58, 27-47.
- Selby, M., 1993. *Hillslope Materials and Processes*-2nd edition. Oxford University Press, NewYork.
- Uytenbogaardt, W., Burke, E.A.J., 1985. *Tables for microscopic identification of ore minerals*. Dover Publications, NewYork.
- Verwaal, W., Mulder, A., 1993. Estimating rock strength with the equotip hardness tester. Elsevier, pp. 659-662.
- Wilkin, R., Barnes, H., 1997. Formation processes of framboidal pyrite. *Geochimica et Cosmochimica Acta* 61, 323-339.
- Yamasaki, S., Chigira, M., 2011. Weathering mechanisms and their effects on landsliding in

pelitic schist. *Earth Surface Processes and Landforms* 36, 481-494.

Zischinsky, U., 1969. Über Sackungen. *Rock Mechanics and Rock Engineering* 1, 30-52.

ACCEPTED MANUSCRIPT

Figure 1

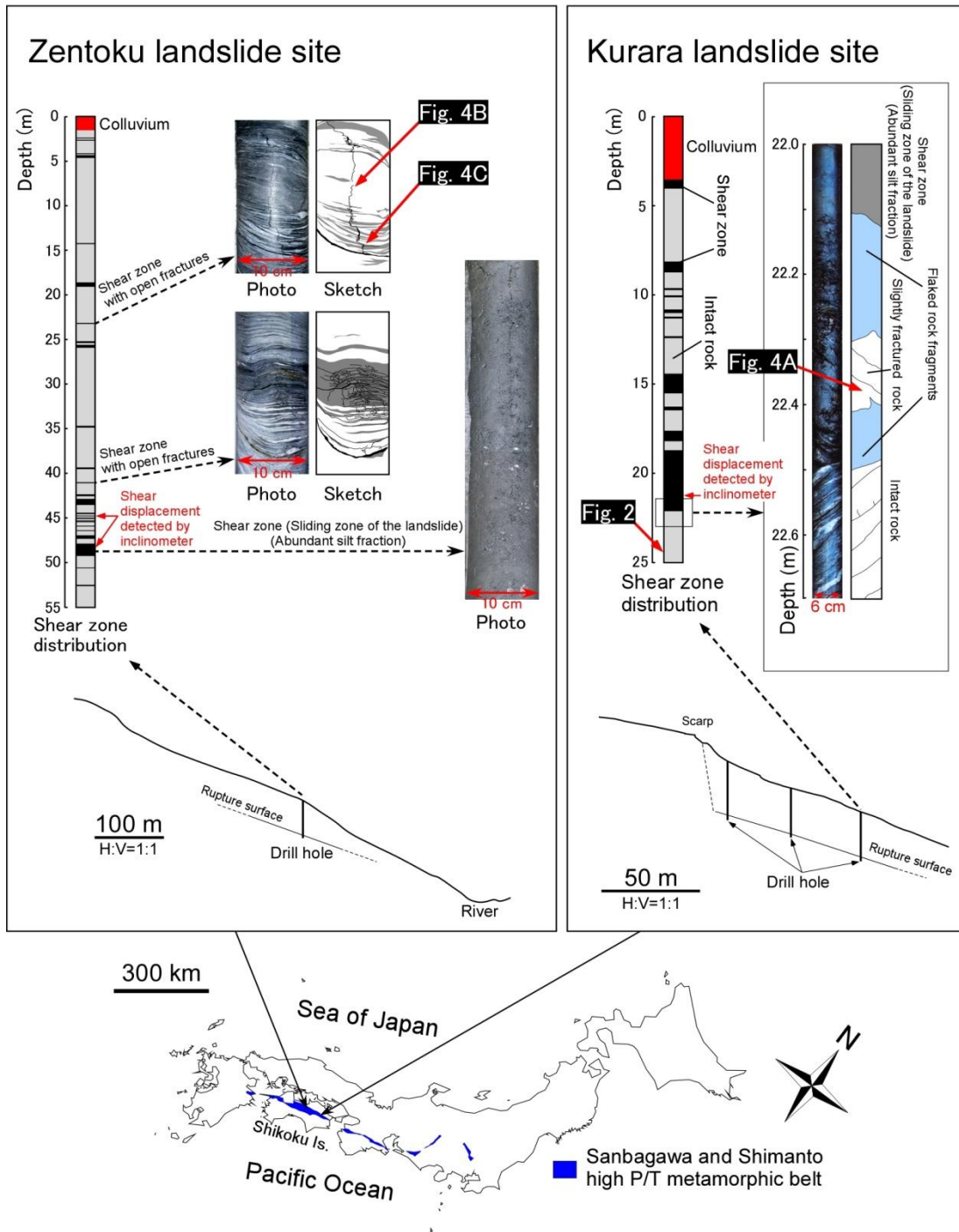


# Figure 2

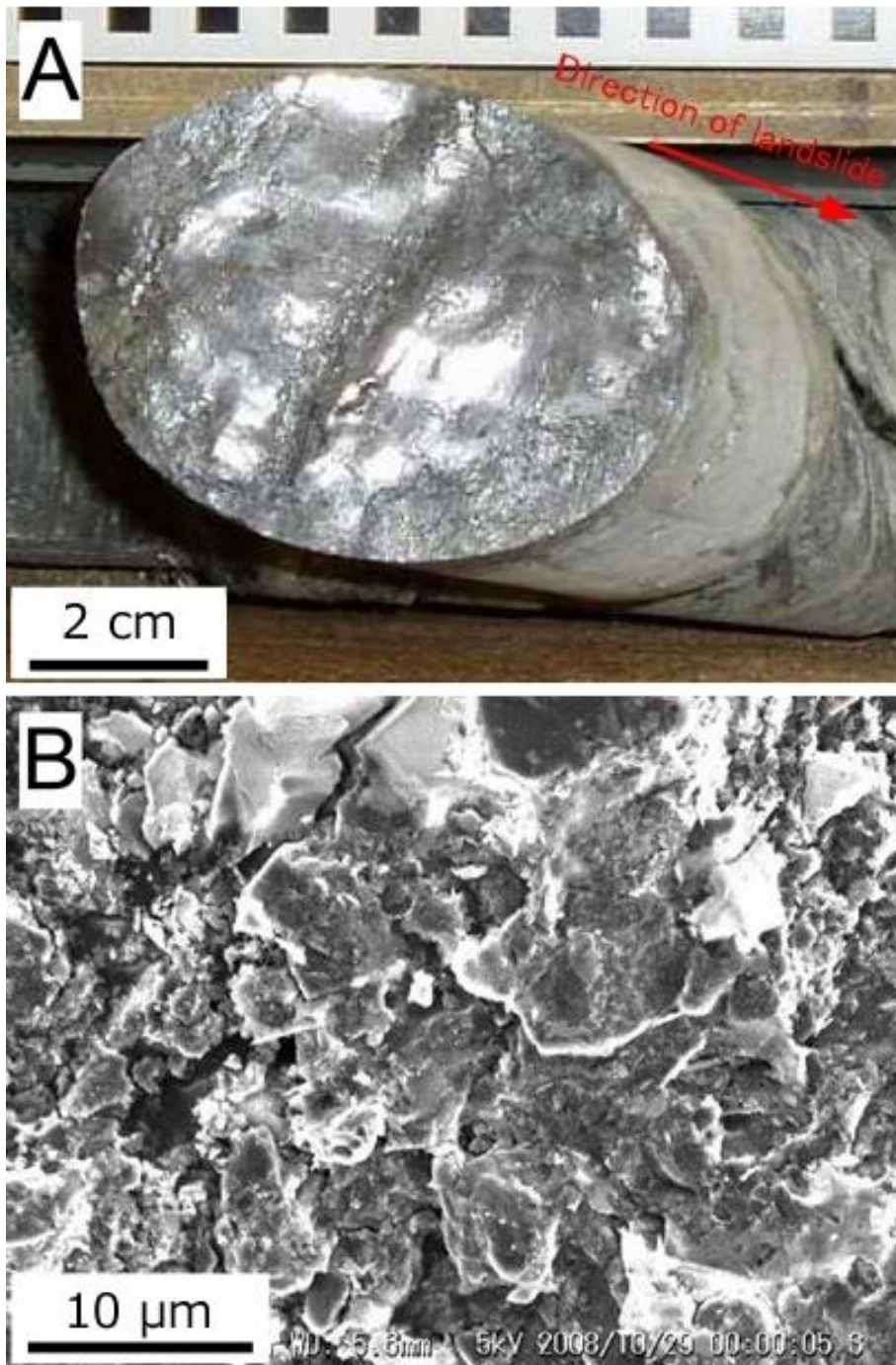


Figure 3

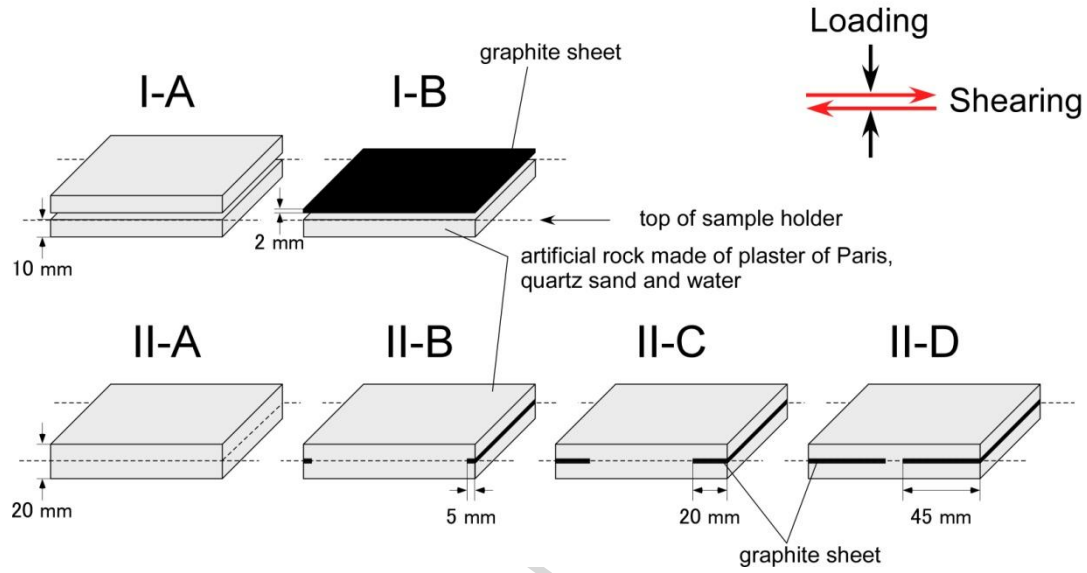


Figure 4

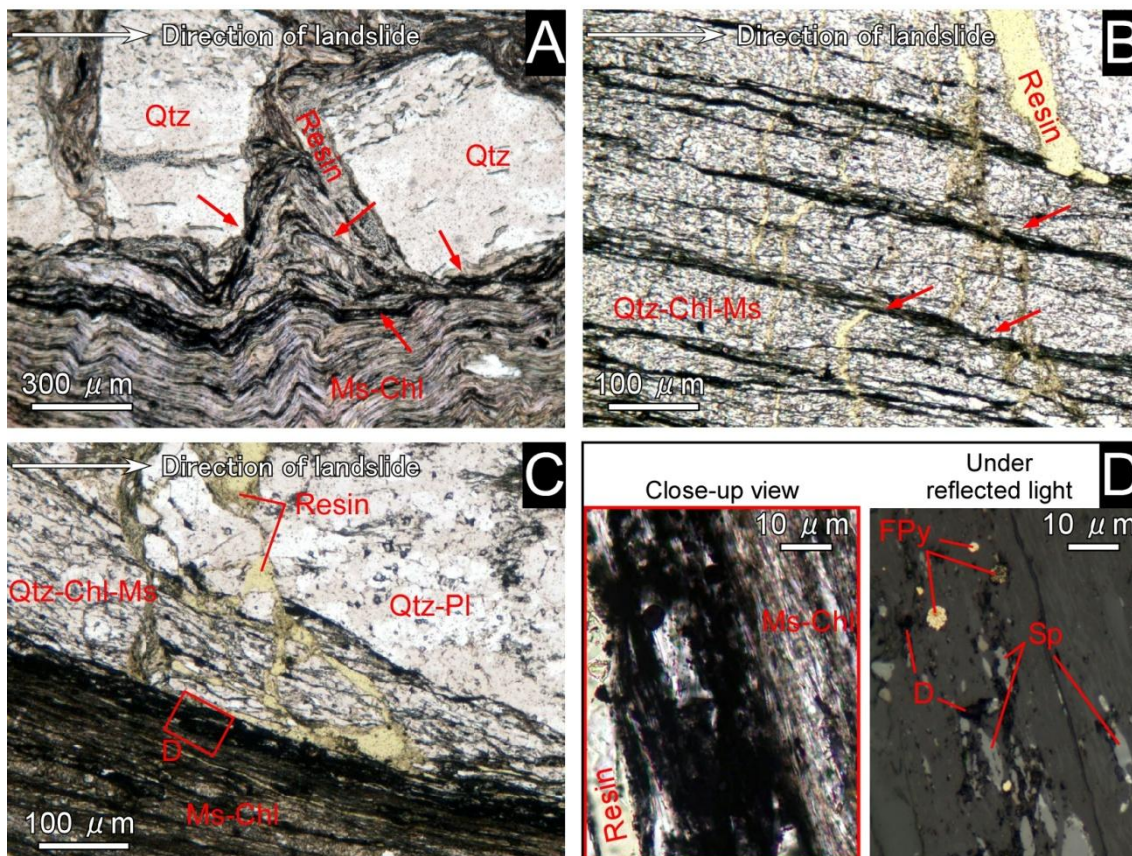
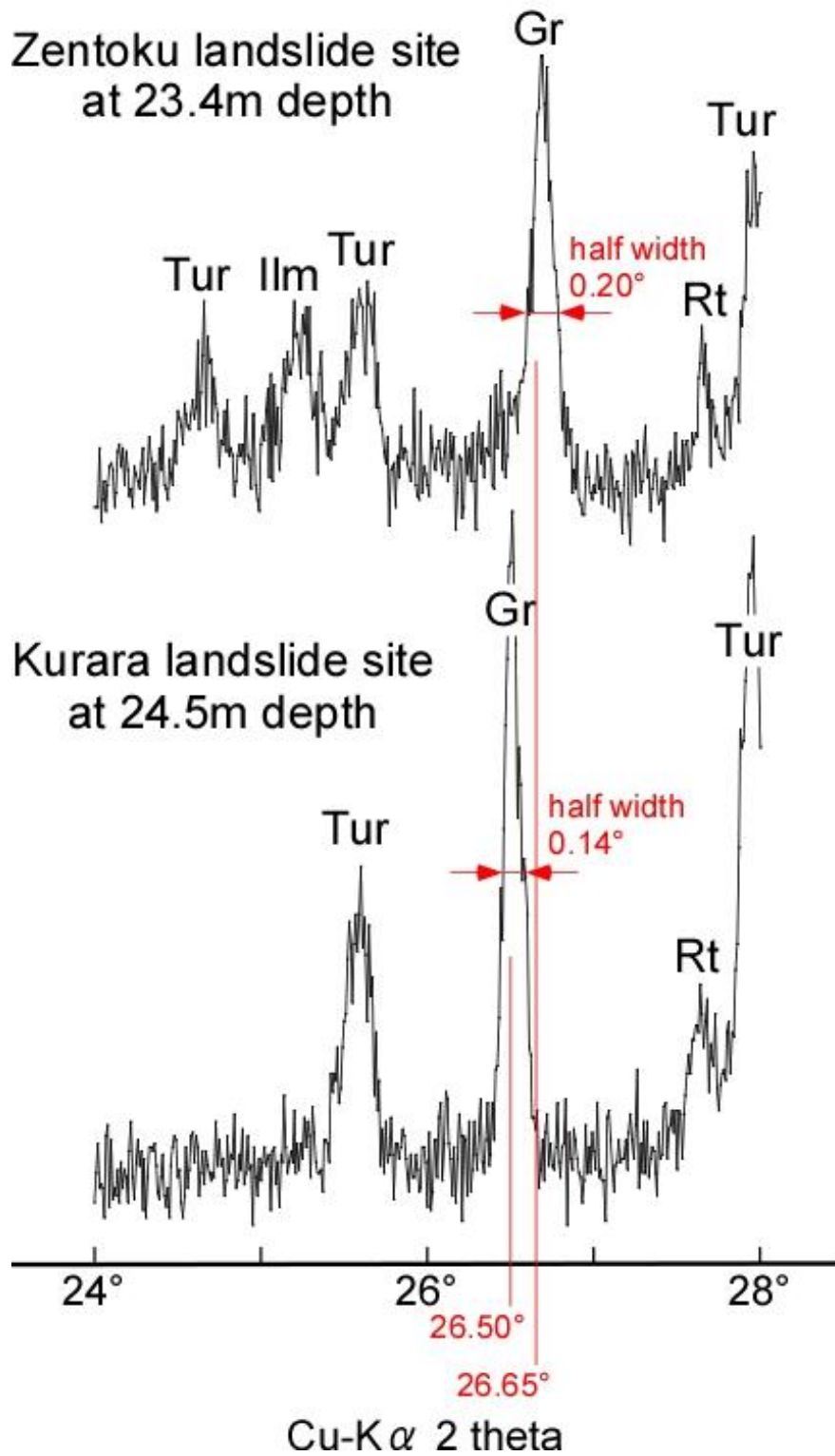


Figure 5



ACCEPTED MANUSCRIPT

Figure 6

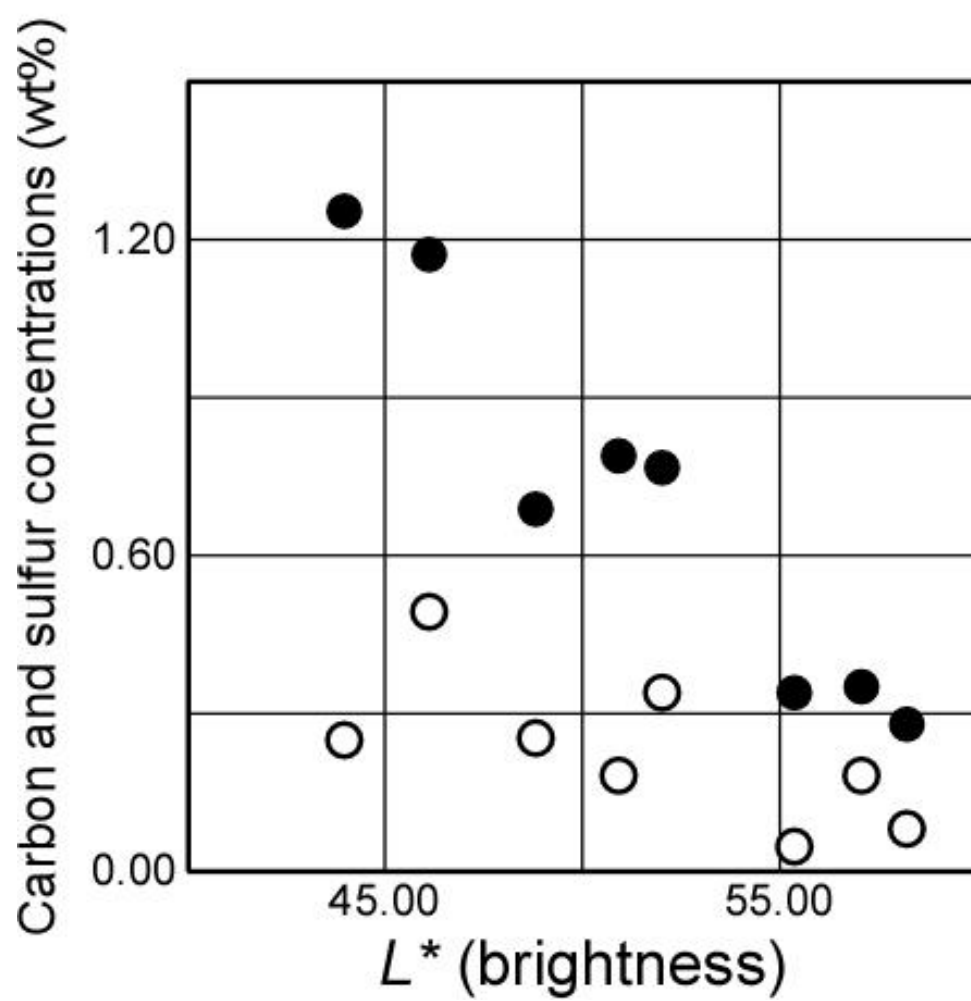


Figure 7

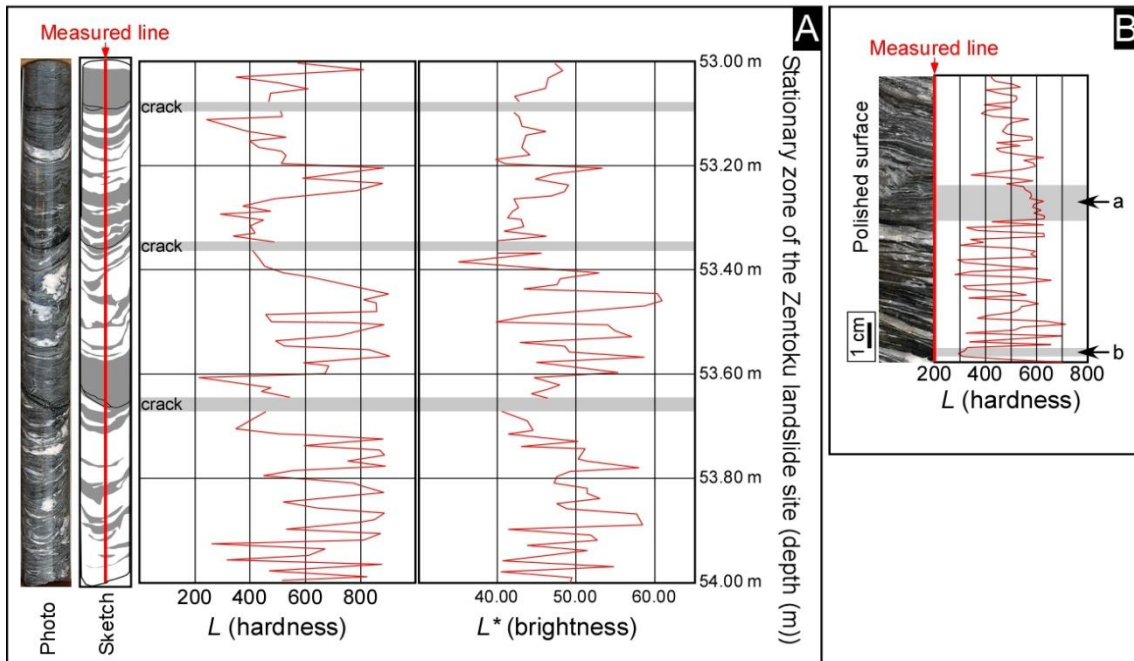


Figure 8

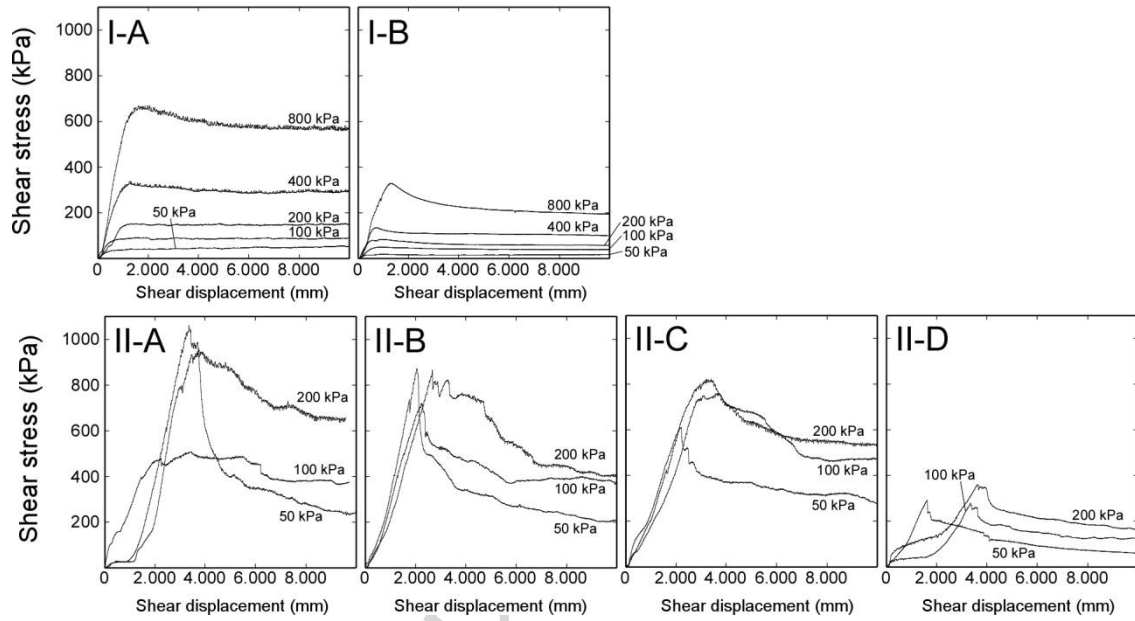


Figure 9

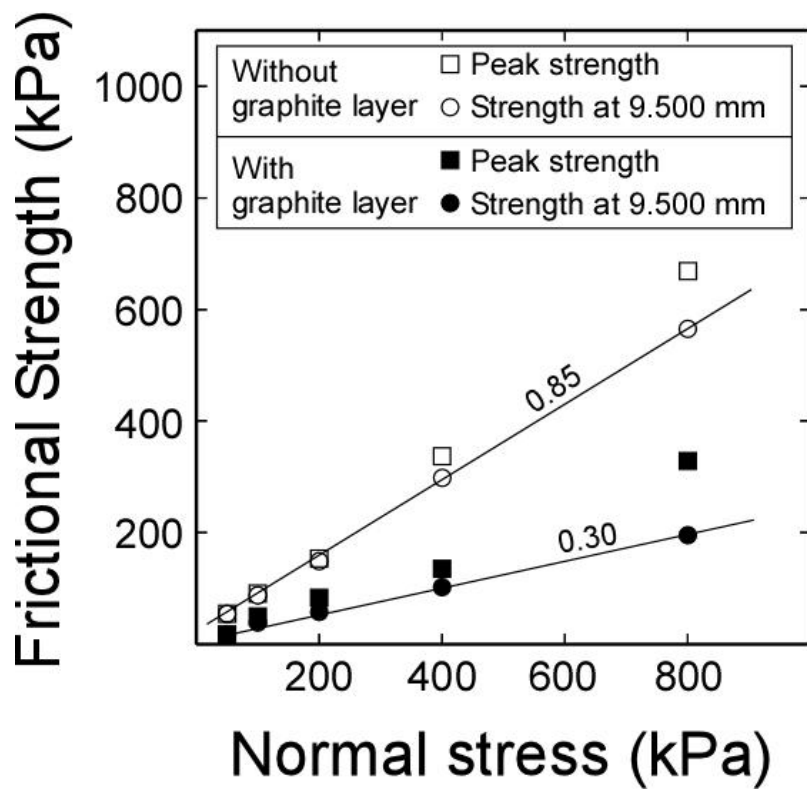


Figure 10

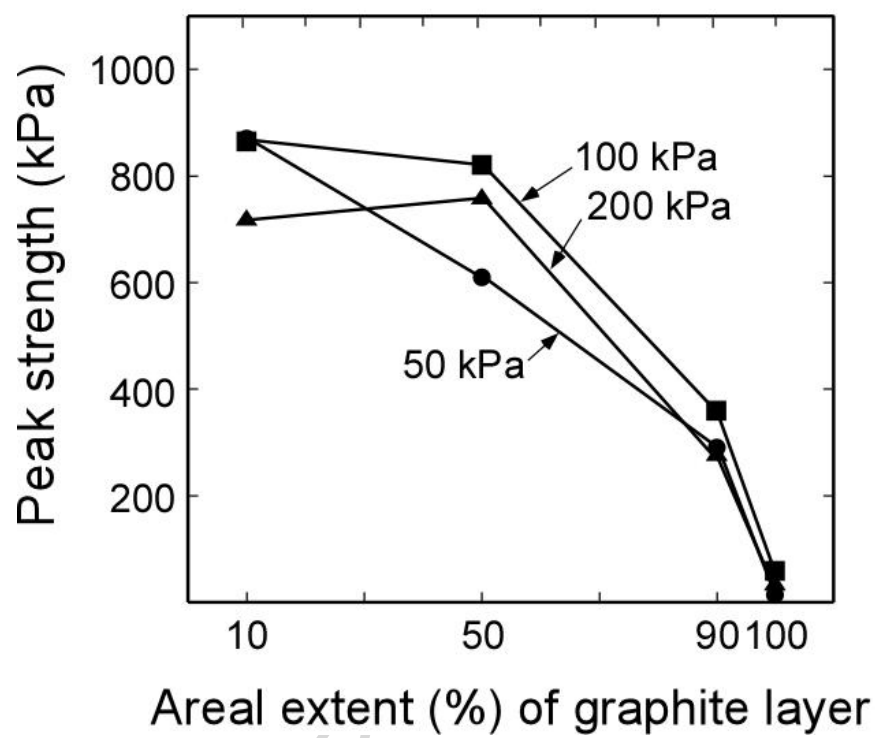


Fig.11

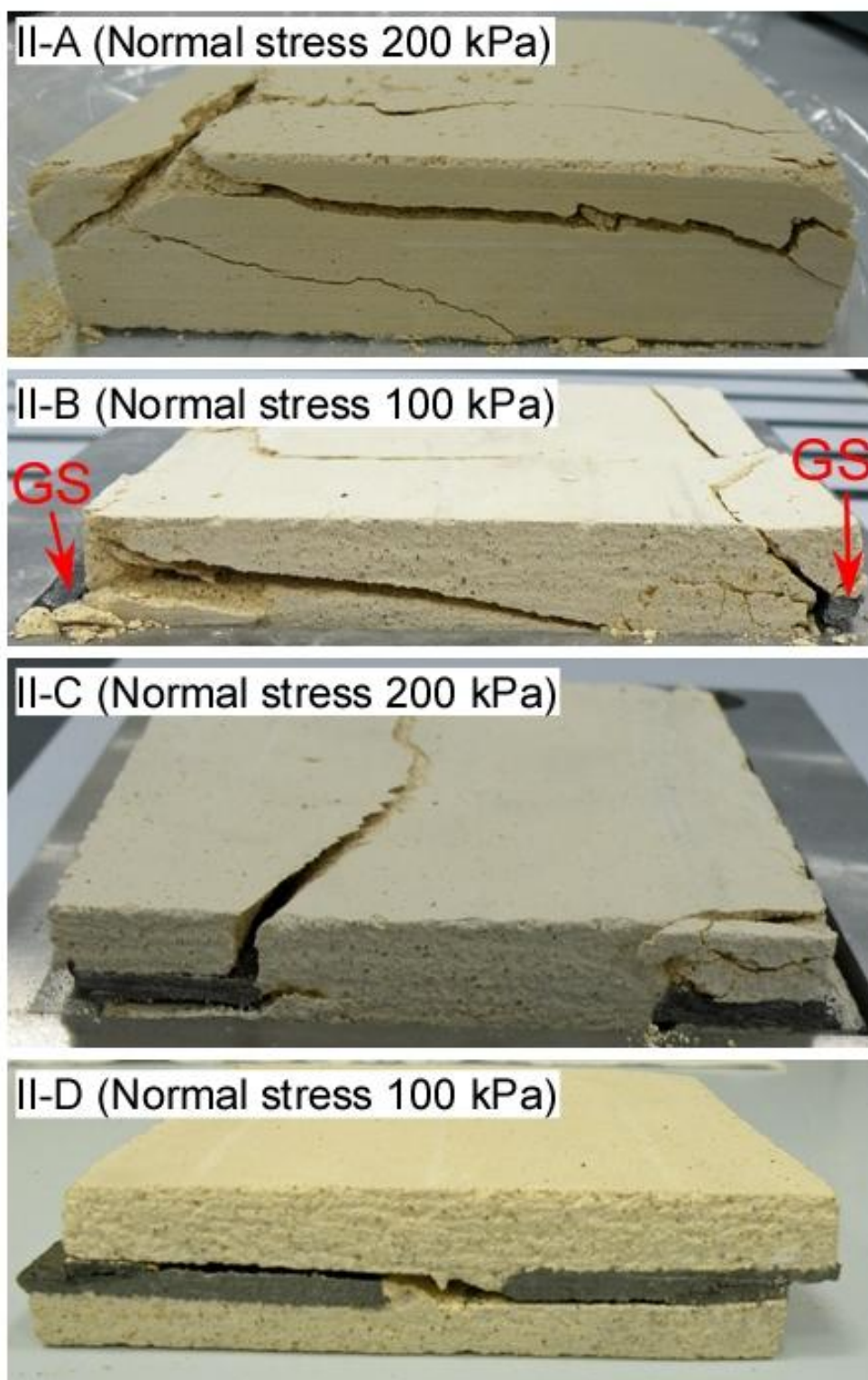


Table 1

Results of color analyses and carbon and sulfur contents of powdered pelitic schist.

Locality	Depth (m)	Color value			Carbon (wt%)	Sulfur (wt%)
		$L^*$	$a^*$	$b^*$		
Kurara	22.4	44.09	-1.25	-2.15	1.25	0.26
	22.5	55.43	-0.93	2.36	0.34	0.02
	22.6	48.81	-1.15	-0.32	0.69	0.27
Zentoku	53.4	58.24	-0.99	3.37	0.28	0.04
	53.5	52.05	-0.75	0.47	0.77	0.33
	53.6	45.99	-1.12	-1.57	1.17	0.53
	53.7	57.16	-1.06	1.17	0.35	0.17
	53.8	50.93	-0.84	0.63	0.79	0.17

Table 2

Results of shear tests of artificial rock samples with and without carbon sheets in shear plane.

Test No.	Series and sample configuration (see Fig. 3)	Normal stress (kPa)	Total shear displacement (mm)	Peak strength (kPa)	Strength at steady state* (kPa)	Vertical displacement at end of test** (mm)	Ruptures formed
1	I	50	10.000	55.501	53.920	0.030	
2		100	10.000	91.037	87.511	0.066	
3		200	10.000	153.684	149.412	0.078	—
4		400	10.000	336.793	298.765	0.114	
5		800	10.000	669.706	565.617	0.182	
6	II	50	10.000	18.579	17.236	0.048	
7		100	10.000	49.803	38.674	0.017	
8		200	10.000	83.794	58.342	0.066	—
9		400	10.000	135.341	102.428	0.114	
10		800	10.000	328.344	196.011	0.153	
11	A	50	10.000	1060.680		-4.085	One or two
12		100	9.714	508.525	-	-2.422	rupture
13		200	9.569	957.677		-2.842	surfaces

14		50	10.000	870.878		-4.592	formed
15	B	100	10.000	720.592	-	-4.221	oblique to
16		200	10.000	865.538		-3.144	shear
17		50	10.000	609.958		-7.321	direction
18	C	100	10.000	760.478	-	-5.263	
19		200	10.000	821.259		-2.130	
20		50	10.000	290.686		-6.976	Single
21		100	10.000	279.149	-	-0.748	rupture
							surface
	D						formed
22		200	10.000	359.340		-0.674	along
							graphite
							layer

### Highlights

- Microscopic slips in pelitic schist occur within thin graphite-rich layers.
- Continuous graphite layer has a considerable effect on shear resistance.
- Graphite rich zones are concentrated locally in pelitic schist area.
- Graphite rich zone could be important for the development place of landslide.